

Neural responses to binocular in-phase and anti-phase stimuli

Bruno Richard¹, Daniel H. Baker²

¹Department of Math and Computer Sciences, Rutgers University, Newark, New Jersey, USA

²Department of Psychology, University of York, York, UK

Abstract

Binocular vision fuses similar inputs from the two eyes into a single percept, whereas incompatible inputs can produce rivalry, lustre, or diplopia. We measured neural responses to binocular stimuli with different phase relationships to test predictions from contemporary models of binocular combination. Steady-State Visually Evoked Potentials (SSVEPs) were recorded from 15 observers in response to monocular and binocular stimulation at 3 Hz, using either On/Off or counterphase flicker with varied spatial and temporal phase relationships. Both On/Off and counterphase flicker elicited responses at the expected fundamental frequency (3 Hz and 6 Hz, respectively) and their harmonics. Manipulating phase relationships modulated these response patterns, including a reduction in the fundamental amplitude for On/Off flicker. The data were modeled with a series of binocular combination algorithms, ranging in complexity from a simple linear sum to a two-stage binocular gain-control model with parallel monocular and binocular phase-selective channels. We found that the model required parallel monocular channels to account for our data, whereas phase selectivity was not essential. Overall, the two-stage contrast gain-control model remains a powerful and flexible framework for describing binocular combination across a wide range of experimental conditions and modalities.

Introduction

The human visual system integrates input from both eyes to form a unified binocular representation of the world. Combining monocular inputs enhances sensitivity to the presented stimuli, particularly when the contrast is low or near detection threshold (Baker et al., 2018; Campbell and Green, 1965; Meese et al., 2006). Contrast sensitivity can improve by a factor of $\sqrt{2}$ or more when stimuli are presented binocularly versus monocularly (Baker et al., 2018; Blake and Wilson, 2011; Campbell and Green, 1965; Richard et al., 2018). Notably, the visual system also attempts to combine inputs even when the stimuli presented to each eye are markedly different (i.e., incompatible). In such cases, observers may perceive binocular rivalry (Blake, 1989; Wilson, 2003), diplopia, or visual lustre (Georgeson et al., 2016). Despite differences in perceptual outcomes, computationally, the underlying processes of binocular

combination for compatible and incompatible inputs appear similar (Baker et al., 2007a; Legge, 1984). Human behavioural responses to compatible and incompatible stimuli can be effectively explained by a single psychophysical model that involves nonlinear transduction, followed by summation across monocular and binocular phase-selective channels (Baker et al., 2007a; Baker and Meese, 2007). Here we explore if the integrative processes defined over multiple behavioural tasks are also reflected at the neural level.

It has long been known that stimuli presented binocularly are summed across the eyes. In contrast detection tasks, where stimulus contrast is low, binocular presentation increases sensitivity by approximately $\sqrt{2}$ (Campbell and Green, 1965). This implies that observers require roughly 1.4 times more contrast to detect a monocular stimulus than a binocular one. The binocular improvement in sensitivity is consistent with a non-linearity operating before the signals from the two eyes (C_L and C_R) are combined (Legge, 1984):

$$R_B = C_L^m + C_R^m. \quad (1)$$

Here, the exponent m determines the degree of summation. When $m = 1$, summation is linear, yielding a doubling of sensitivity. When $m = 2$, summation is reduced to $\sqrt{2}$. Several studies have reported summation ratios over $\sqrt{2}$ with some approaching 1.8 (Meese et al., 2006; Simmons, 2005; Simmons and Kingdom, 1998). A recent meta-analysis of 65 studies ($N = 716$) found an average binocular summation ratio of 1.5 (Baker et al., 2018). This work highlighted the challenges in accurately describing the binocular summation process (e.g., m) as individual variability and methodological differences can greatly impact binocular summation.

The contrast of stimuli is crucial in measuring binocular summation. Binocular summation can be very large when stimulus contrast is low; however, the binocular advantage is seldom observed in tasks that involve higher contrasts. In contrast discrimination tasks, where observers judge the contrast difference between otherwise identical stimuli, binocular presentation no longer confers a benefit in sensitivity: discrimination thresholds are identical whether stimuli are shown to one eye or both (Legge, 1984; Maehara and Goryo, 2005; Meese et al., 2006). This is not, however, an indication that binocular summation does not occur at higher contrasts; the monocular signals are still summed (Meese et al., 2006; Meese and Baker, 2011). Instead, the advantage of summation is counteracted by normalization mechanisms that maintain consistency across viewing conditions (referred to as ‘ocularity invariance’). In contrast gain control models of early vision, normalization can stem from interocular and self-suppressive signals (Meese et al., 2006):

$$R_B = \frac{C_L^m}{S + C_L + C_R} + \frac{C_R^m}{S + C_R + C_L}. \quad (2)$$

When both eyes are stimulated, the suppressive terms on the denominators offset the enhanced excitatory signals, nullifying the binocular advantage.

A similar pattern of results is observed in neural measurements of binocular summation. In functional Magnetic Resonance Imaging (fMRI) recordings, neural responses are significantly larger for binocular than monocular responses when stimulus contrast is low (Moradi and

Heeger, 2009). At higher contrasts, observers no longer show the binocular advantage. As with behavioural results, these findings are well-explained computationally by interocular suppression and binocular contrast normalization. The equivalency in binocular summation between psychophysics and neuroimaging findings means that both data types can be used to constrain binocular summation models. We, for example, have previously demonstrated that a popular model of binocular summation could be easily adapted to capture Steady-State Visually Evoked Potentials (SSVEPs) to monocular and binocular stimuli when one eye was occluded by a neutral density filter (Richard et al., 2018). Placing a neutral density filter in front of one eye darkens its input, reducing the amplitude and altering the phase of SSVEPs to stimuli presented to the filtered eye. Steady-State response amplitudes and phases to stimuli presented through different neutral density filter strengths were well described by a model that first used a biophysically plausible temporal filter on the input stimuli, followed by self and interocular suppression, and finally, binocular contrast normalization. This model also explained psychophysically measured binocular summation in the same group of observers. A comprehensive description of the processes involved in binocular summation should be able to explain behavioural and neuroimaging findings under various experimental conditions of binocular summation.

Many studies have worked towards the development of a comprehensive description of the process of binocular summation in human vision using a variety of psychophysical and neuroimaging data (Baker et al., 2008, 2007b; Ding et al., 2013; Ding and Sperling, 2006; Legge, 1984; Lygo et al., 2021; Maehara and Goryo, 2005; May and Zhaoping, 2016; Richard et al., 2018). This is not an insignificant challenge; such a description must account for multiple components of early vision, including identifying relevant signals, defining how these signals might interact, what non-linearities are present, and most importantly, how these signals are summed and/or differenced. One such model that has proven very informative and capable of describing binocular summation under various experimental conditions is the two-stage contrast gain control model developed by Meese et al. (2006). The model captured detection and discrimination thresholds for monocular and binocular in addition to dichoptic (the stimuli presented to both eyes are not identical) stimuli, in a two-stage process. First, the input is rectified by an excitatory non-linearity ($m \approx 1.3$) and normalized by self and interocular suppression (see Equation 2). The binocular (e.g., combined) input undergoes a second contrast normalization before the decision stage,

$$R = \frac{R_B^p}{Z + R_B^q}, \quad (3)$$

where the excitatory exponent p allows for greater increase in sensitivity than would be seen by the excitatory non-linearity of the first stage (m in Equation 2) alone.

Subsequent iterations of the two-stage contrast gain control model added channels for opposite contrast polarities (Baker and Meese, 2007), monocular channels parallel the binocular summing channel (Georgeson et al., 2016). Polarity-specific channels were included to explain masking effects when the stimuli presented to each eye had opposing phase polarities (i.e., dichoptic presentation). The presentation of sinusoidal gratings with opposite polarities to each eye does not cancel them out: the stimuli remain detectable and the two inputs can

sum (Bacon, 1976; Baker and Meese, 2007; Simmons, 2005). Parallel monocular channels were added to account for adaptation after-effects that suggest monocular signals may be preserved and available for perception following binocular summation (Blake et al., 1981; Moulden, 1980).

While the possibility of monocular channels had been considered (Legge, 1984), many assumed that only the binocularly summed signal contributed to perception. Georgeson et al. (2016) developed a specific experimental condition to assess the involvement of monocular channels. They devised a discrimination task where the target interval presented a contrast increment to one eye (e.g., 10% pedestal + 2%) and a contrast decrement to the other (e.g., 10% pedestal - 2%). If the only available signal is a binocularly summed one, the task would be nearly impossible to complete; the target interval would be perceptually identical to the pedestal-only interval. However, observers were able to complete the task. The two-stage contrast gain control model with parallel monocular channels was the only model able to capture observer thresholds from all experimental conditions, including the binocular increment and decrement tasks. There has also been accruing evidence of an additional differencing channel that accompanies the summing channel commonly described in binocular combination (Chen and Li, 1998; May et al., 2012; May and Zhaoping, 2016). This channel, as the name implies, encodes the difference between stimuli presented to the left and right eye; early contributions to disparity processing and stereovision. While computational models of binocular vision do not explicitly include differencing channels, encoding the difference between monocular signals is, indirectly, included in the two-stage contrast gain control model defined by Georgeson et al. (2016).

The current architecture of the two-stage contrast gain control model has been rigorously evaluated on psychophysical data, providing a solid foundation for our understanding of binocular combination (Baker and Meese, 2007; Georgeson et al., 2016; Meese et al., 2006). While previous studies have utilized the two-stage contrast gain control model on neuroimaging data (Lygo et al., 2021; Richard et al., 2018), they only included experimental conditions where the phases of the sinusoidal gratings presented to each eye were identical. To accurately assess the current architecture of the two-stage contrast gain control model, neuroimaging data for binocular presentation of stimuli in opposite phase polarity are required. Here, we recorded SSVEPs to monocular and binocular stimuli with different spatial and temporal phase relationships to obtain the data needed to evaluate the two-stage contrast gain control model. By progressively increasing the complexity of the model, we demonstrate that many mechanisms of binocular combination, such as monocular non-linearities, interocular interactions, and parallel monocular channels, are required to explain neural responses to our set of experimental conditions. The two-stage contrast gain control model remains a powerful and flexible descriptor of the architecture of binocular combination for data collected across many experimental conditions and modalities.

Methods

Participants

Fifteen observers (including both authors: BR and DHB) with normal or corrected to normal visual acuity and binocular vision participated in our study. Written informed consent was obtained from all participants, and experimental procedures were approved by the ethics committee of the Department of Psychology at the University of York.

Apparatus

All stimuli were presented using a gamma-corrected ViewPixx 3D display (VPixx Technologies, Canada) driven by a Mac Pro. Binocular separation with minimal crosstalk was achieved by synchronizing the display’s refresh rate with the toggling of a pair of Nvidia stereo shutter goggles using an infrared signal. The monitor refresh rate was set to 120 Hz; each eye updated at 60 Hz (every 16.67 msec). The display resolution was set to 1920 X 1080 pixels. A single pixel subtended 0.027° of visual angle (1.63 arc min) when viewed from 57 cm. The mean luminance of the display viewed through the shutter goggles was 26 cd/m².

EEG signals were recorded from 64 electrodes distributed across the scalp according to the 10/20 EEG system (Chatrian et al., 1985) in a WaveGuard cap (ANT Neuro, Netherlands). We monitored eye blinks with an electrooculogram consisting of bipolar electrodes placed above the eyebrow and the cheek on the left side of the participant’s face. Stimulus-contingent triggers were sent from the ViewPixx display to the amplifier using a parallel cable. Signals were amplified and digitized using a PC with the ASALab software (ANT Neuro, Netherlands). All EEG data were imported into MATLAB (Mathworks, MA, USA) using components of the *EEGlab* toolbox (Delorme and Makeig, 2004) and then exported for subsequent offline analysis using R.

Stimulus Creation

Observer SSVEPs were measured with a single horizontal sinusoidal grating that subtended 15° of visual angle on the retina with a spatial frequency of 3 cycles/ $^\circ$ of visual angle (Figure 1A). Our experimental conditions modulated the interocular spatial phase of stimuli (Figure 1A). Under binocular viewing, the sinusoidal gratings could be presented in spatial phase or spatial anti-phase. When stimuli were presented in spatial phase, the aligned sinusoidal gratings were identical in both eyes ($\Delta\phi = 0$). The spatial anti-phase condition phase-shifted one of the sinusoidal gratings by 180° ($\Delta\phi = \pi$). Stimuli were also modulated in their oscillatory pattern, which could be On/Off or counterphase flicker at a frequency of 3Hz (Figure 1B). Under On/Off contrast flicker, the relative contrast of the gratings began at 0%, increased smoothly to 100% of the nominal maximum (100% Michelson contrast), and then returned to 0% over 333 ms (i.e., one cycle). On/Off flicker will generate SSVEPs at the fundamental frequency (3Hz) and its integer harmonics (2F, 3F, 4F, see Figure 1C). Counterphase flicker reversed the phase of the gratings at a frequency of 3Hz. The contrast of the grating began at the relative maximum (100%), gradually decreased in contrast to 0% of the relative maximum, and then increased again to 100% but in the opposite phase

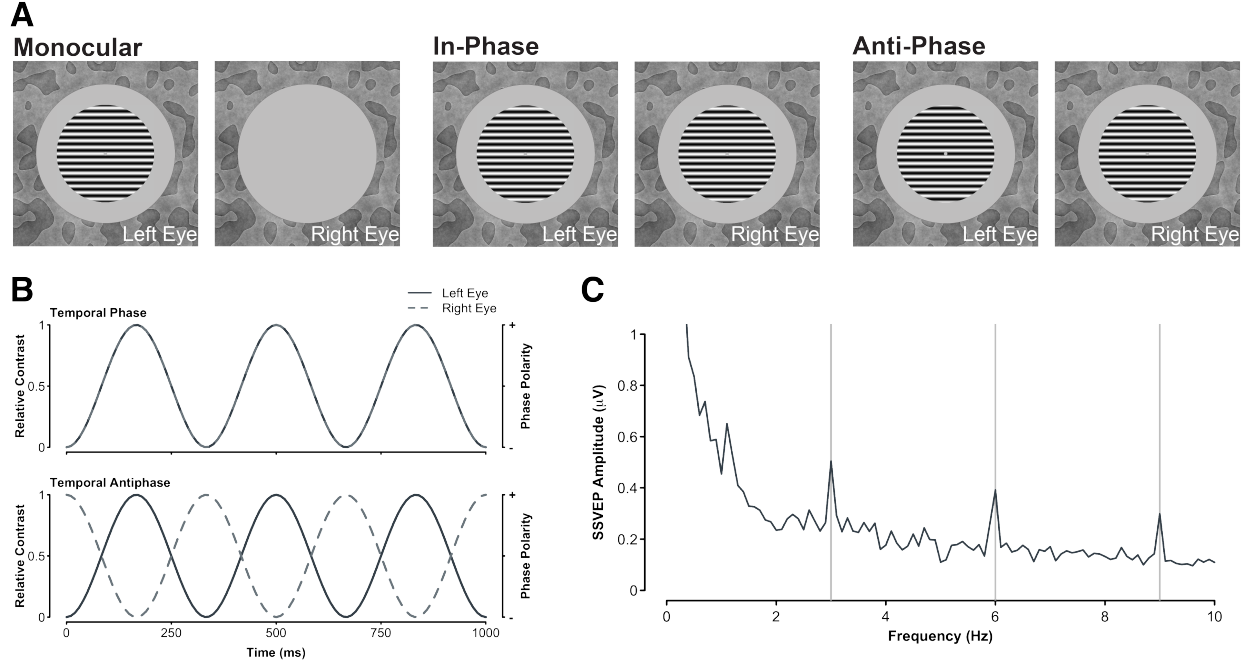


Figure 1: **A.** The spatial configuration of stimuli presented to observers in our experiment. Monocular conditions presented the sinusoidal grating to the left or right eye of observers (counterbalanced) while the other eye was presented with a gray screen set to mean luminance. Binocular conditions could be shown with stimuli in spatial phase, whereby the phase of both sinusoidal gratings was identical, or in spatial anti-phase, where the phase of the sinusoidal gratings presented to each eye was opposite. The background texture did not change throughout the trial to aid with binocular fusion. **B.** The temporal configuration of our stimuli. To generate SSVEPs, stimuli were contrast modulated in two ways: on/off (left Y axis) or counterphase (right Y axis). The oscillatory pattern could also be in phase (upper plot), where both stimuli were modulated in the same manner, or in counterphase (lower plot), where as one stimulus increased in contrast, the other decreased in contrast (or increased in opposite polarity). **C.** Example SSVEPs generated under binocular spatial and temporal in-phase viewing of stimuli for one observer, with an average of four electrodes (Oz , POz , $O1$, $O2$) and 12 repetitions.

polarity. Unlike On/Off flicker, counterphase flicker generates two nearly identical transients per cycle and thus does not produce SSVEPs at the fundamental frequency (3Hz) but only its even harmonics (Wade and Baker, 2025).

To aid with binocular fusion, stimuli were surrounded by a static binocular texture presented beyond the central 19° stimulus aperture. These textures were constructed by first low-pass filtering a white (amplitude $\propto 1/f^0$) noise pattern, dichotomizing its output into a binary image and taking its phase spectrum. A second flat (amplitude $\propto 1/f^0$) was adjusted by multiplying each spatial frequency’s amplitude coefficient by f^{-1} to generate a pink amplitude spectrum (Hansen and Hess, 2006; Tadmor and Tolhurst, 1994). The pink amplitude spectrum and the phase spectrum of the binary image were rendered in the spatial domain by taking the inverse Fourier transform, resulting in the pattern shown in Figure 1A.

Procedures

Steady-State Visually Evoked Potentials (SSVEPs) were recorded with monocular and binocular stimulation using either on-off or counterphase flicker at 3Hz. Across the eyes, binocular stimuli could be in spatial and temporal phases, in temporal phase but spatial anti-phase, in spatial phase but temporal anti-phase, or spatial and temporal anti-phase (on-off flicker only). Stimuli presented in spatial and temporal anti-phase under counterphase flicker are identical to stimuli presented in spatial and temporal phase (and so we did not duplicate this condition). Thus, this experiment was comprised of a total of nine conditions - two monocular and seven binocular - which were each repeated 12 times for a total of 108 trials. Stimulus presentation was separated into four experimental blocks, each containing 27 trials. A trial lasted 15 seconds; a grating stimulus flickered onscreen for 11 seconds, followed by a screen with its central 19° set to mean luminance for 4 seconds. Participants completed all 27 trials of an experimental block in a single sequence (6.75 minutes) and were given breaks between experimental blocks. The trial order was pseudo-randomized on each block. Participants did not receive explicit task instructions other than to fixate the marker in the center of the display and blink only during the blank period between stimulus presentations.

SSVEP Analysis

We used whole-head average referencing to normalize each electrode to the mean signal of all 64 electrodes (for each sample point). The EEG waveforms were Fourier transformed at each electrode for a 10-second window, beginning one second after the stimulus onset to avoid onset transients. The Fourier spectra were coherently averaged (i.e., retaining the phase information) across four occipital electrodes (Oz , POz , $O1$ and $O2$) and trial repetitions (see Figure 1C). We then calculated signal-to-noise ratios (SNRs) by dividing the absolute amplitude in the signal bin (e.g., 3 Hz) by the mean of the absolute value of the ten adjacent bins (± 0.5 Hz in steps of 0.1 Hz). Given that distributions of SNRs are inherently skewed, the median SNR was taken across all participants; the median is a more robust descriptor of central tendency in skewed distributions.

Results

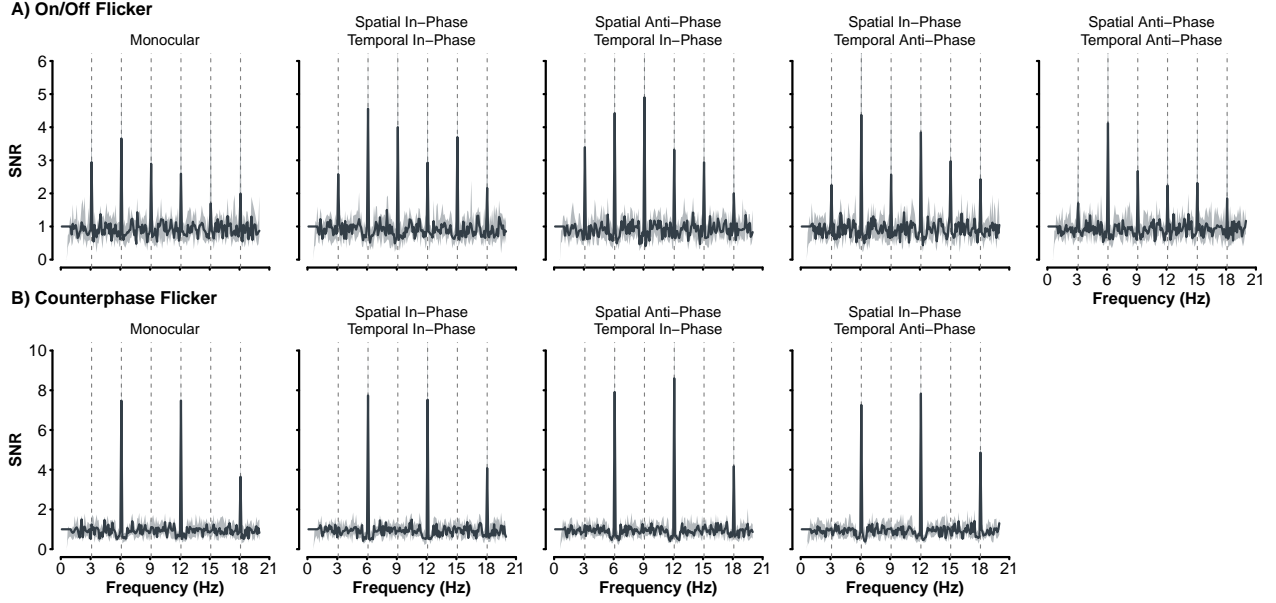


Figure 2: Cross-participant median SNRs for frequencies up to 20Hz. SNRs generated by On/Off flicker are shown in the top row (A), while those generated by counterphase flicker are shown in the bottom row (B). The light gray area represents 95% bootstrap confidence intervals that were calculated by resampling (with replacement) participant SNRs 2000 times.

Figure 2 shows the cross-participant median SNR spectra for all experimental conditions. Responses for all On/Off flicker experimental conditions generated peaks at the fundamental frequency (3Hz) and its harmonics (integer multiples of 3Hz). Similarly, counterphase flicker produced responses at twice the flicker frequency (6 Hz) and its harmonics. We assessed differences in SNR magnitude across experimental conditions via a permutation test, which allows for a non-parametric comparison of a statistic between two conditions. To conduct the permutation tests, we first take the median difference between two experimental conditions (i.e., the observed difference). A null distribution is then constructed by combining SNR values from both experimental conditions, and randomly sampling them without replacement to create two groups of sizes identical to their original, but with values that are not associated with a particular experimental condition. The median difference of the randomly sampled SNRs is then taken. This process is repeated multiple times (e.g., $N = 2000$) to build a distribution of median differences with no association of experimental condition (i.e., a null-hypothesis distribution). The observed median difference is then compared to this distribution. The proportion of scores greater than the observed difference represents the p value associated with the test. When comparing SNRs at the fundamental frequency (3Hz) for On/Off flicker, we find no statistically significant difference in median SNR magnitude between experimental conditions where stimuli were presented in temporal phase (see Figure 3). Monocular and binocular presentation for stimuli presented in temporal phase resulted in a similar response pattern under both On/Off and counterphase flicker modulations. This is consistent with ocularity invariance; binocular and monocular stimuli are judged equal in magnitude at high contrast (Baker et al., 2018; Legge, 1984; Maehara and Goryo, 2005;

Meese et al., 2006).

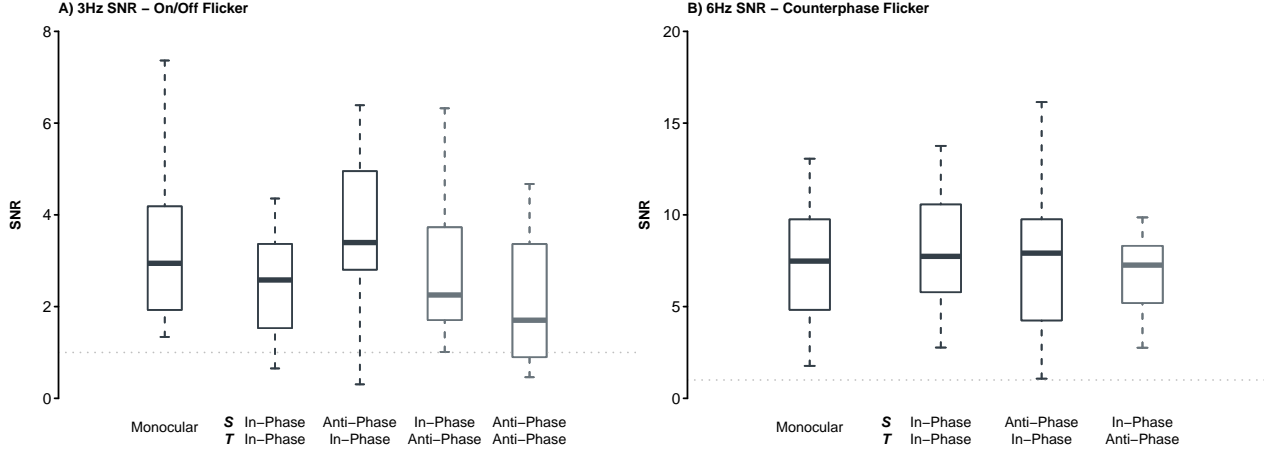


Figure 3: Boxplots of participant SNRs at the fundamental frequency for each experimental condition in our study. A) Boxplots represent the participant SNR at 3Hz. The median SNR is shown by the thick line within the box, with the lower and upper border of the box representing the first (25%) and third (75%) quartile of the SNR distribution. Dashed lines show the lower and upper whisker limits, which are calculated as 1.5 times the interquartile range (distance between the third and first quartile). Boxplots for the binocular conditions have labels for their spatial (S) and temporal (T) phase relationships. Experimental conditions where stimuli are presented in temporal anti-phase are shown in a lighter gray. B) As in A, boxplots show participant SNRs at 6Hz, the fundamental frequency for counterphase flicker. In both graphs, the dashed line represents an SNR of 1.0.

Changing the phase relationships of stimuli under On/Off flicker had some interesting impacts on the fundamental frequency (Figure 3A). Stimuli presented in spatial phase and temporal anti-phase generated smaller SNRs ($\text{median}_{\text{SNR}} = 2.25$) than stimuli presented in spatial anti-phase and temporal phase ($\text{median}_{\text{SNR}} = 3.40$, $p = .047$). The reduction in the amplitude relative to stimuli in spatial anti-phase and temporal phase was also observed for stimuli in temporal and spatial anti-phase ($\text{median}_{\text{SNR}} = 1.70$; $p = .023$). No other statistically significant difference in median SNRs were observed for all counterphase flicker conditions or the other harmonics for On/Off flicker (all p values were greater than .05). While the median SNRs under On/Off flicker shown in temporal anti-phase were reduced in comparison to other conditions, both the spatial in phase temporal anti-phase condition ($p < .001$) and the spatial and temporal anti-phase conditions ($p = .004$) had median SNR values that were statistically significantly greater than 1.0. The presence of a 3Hz response for binocular stimuli presented in temporal anti-phase indicates that monocular responses remain and contribute to the SSVEP, as these conditions generate two transients per cycle and a purely binocular signal would only generate responses at 6Hz (Blake et al., 1981; Georgeson et al., 2016; Moulden, 1980).

Modelling

The perception of stimulus contrast across eyes is well-explained by psychophysical models that process input contrast in two sequential contrast gain control stages interposed by binocular summation (Baker et al., 2008, 2007a, 2007b; Baker and Meese, 2007; Meese et al.,

2006). This simple, yet powerful, family of models not only captures behavioural data well, but can also explain neural responses to binocular and dichoptic stimuli (Baker and Wade, 2017; Lygo et al., 2021; Richard et al., 2018). Our SSVEP results show the expected pattern of binocular combination for stimuli presented at high contrast (i.e., ocularity invariance) but also intriguing effects that are likely explainable by the most recent extension of the two-stage contrast gain control model, as defined in Georgeson et al. (2016). To explore the architecture required to describe our effects adequately, we progressively increase the complexity of binocular combination beginning with a wrong model (i.e., linear combination) and building up to a multi-channel model with monocular, binocular and phase-selective pathways (Figure 4).

**Two-Stage Contrast Gain Control Model with
Parallel Monocular and Phase-Selective Channels (Left Eye)**

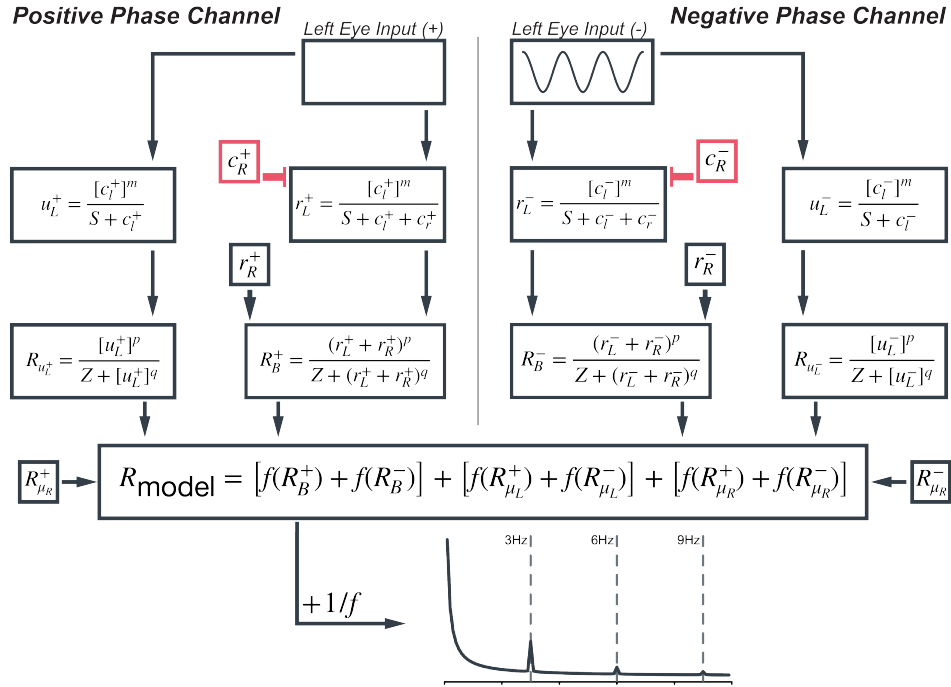


Figure 4: The multi-channel variant of the two-stage contrast gain control model. This diagram shows the channels for the left eye. Contributions from the right eye (c_R^+ and r_R^+) to the binocular channels are shown in small boxes. Unlike the model defined by Georgeson et al. (2016), responses from the parallel monocular channels are added to those of the binocular channels before signal selection for phase-selective channels. This change accounts for methodological differences when fitting neuroimaging data. To fit the final response of the model, R , was Fast Fourier Transformed, and a pink noise spectrum was added to allow for a comparable calculation of model SNRs as is done with human data.

The architecture of the models explored differs, but all received the same input and had their final outputs processed identically. The input to all models was a 3 Hz sine wave, adjusted to accurately represent the various experimental conditions of this study (see Figure 1). For example, stimuli presented with On/Off flicker in temporal anti-phase had the left eye

input generated by the following equation,

$$c_L = A * (\cos(2\pi ft) + 1)/2, \quad (4)$$

while the right eye input would be defined as,

$$c_R = A * (-\cos(2\pi ft) + 1)/2. \quad (5)$$

A represents stimulus contrast (amplitude), f the temporal flicker frequency (i.e., 3 Hz), and t time in milliseconds. The input to the other eye (c_R) is phase shifted by 180° , which can be accomplished using the negative cosine function ($-\cos$). Finally, sine waves are rectified to range between 0 and 1 to represent the relative contrast presented to observers. The same experimental condition with counterphase flicker has the following sinusoidal profile for the left eye,

$$c_L = A * [\cos(2\pi ft)]_+ \quad (6)$$

and for the right eye,

$$c_R = A * [-\cos(2\pi ft)]_+. \quad (7)$$

These profiles are identical to the On/Off flicker, but the sine waves are half-wave rectified to represent the counterphase oscillation. To fit model outputs (rectified sine waves) to observer data, the final response of the models was Fast Fourier Transformed, and a pink noise spectrum was added to the Fourier amplitude, $|FFT(R_{\text{model}})| + 1/f$, before calculating model SNRs. All models developed in this study were fit by minimizing the sum of squared errors between the model output and the observer median SNRs for the first 6 SSVEP components (3Hz, 6Hz, 9Hz, 12Hz, 15Hz, and 18Hz).

Evidently wrong models

As a first step in defining the necessary architecture to capture our results, we built wrong models with no monocular stage or phase selectivity. The first is a purely linear summation model of binocular combination,

$$R_B = c_L + c_R, \quad (8)$$

the binocular response (R_B) is the sum of the monocular inputs. The fits of the linear summation model are shown in Figure 5 and its performance metrics in Table 1. For On/Off flicker, the linear summation model only generates responses at the fundamental frequency (3Hz) that grossly overestimate observer SNRs. This is expected as this model lacks the rectification and non-linearities required to generate responses at the harmonics (Regan and Regan, 1988; Wade and Baker, 2025). In a linear sum, stimuli presented under On/Off flicker in temporal anti-phase cancel each other, and thus the model generates no response. The model does generate responses at the fundamental and harmonics of the counterphase flicker condition (Figure 5B), but this is attributable to the input's rectification (the half-wave rectification applied to the input; Equation 6, Equation 7) and not the model architecture.

Model	R^2	RMSE	AIC
Linear sum	-	3.234	281.99

Model	R^2	RMSE	AIC
Linear sum, with Rectification	0.575	1.405	197.95
Two-Stage, no interocular interactions	0.822	0.908	154.86
Two-Stage, with interocular interactions	0.81	0.94	158.62
Two-Stage with parallel monocular channels	0.877	0.756	135.1
Two-Stage with phase-selective channels & monocular channels	0.876	0.759	135.39

Table 1: Goodness-of-fit metrics for all models compared in this study. Errors in predictions for the linear sum model were too large to calculate R^2 . RMSE is the Root Mean Square error and AIC is the Aikake Information Criterion.

Responses of neurons to contrast in the visual system are well-modeled by a saturating non-linearity: as contrast increases, the magnitude of responses saturates (the increase in response per unit contrast decreases at higher contrast values; Heeger (1992)). The saturating non-linearity can be modeled in different ways, but generally contains a divisive suppression and an exponentiation of the excitatory and inhibitory inputs. The inclusion of suppression can aid the model in better capturing the magnitude of responses in our observers while exponents introduces the non-linearities required to generate responses at the harmonic frequencies. Thus, the next increment in our model complexity defines the binocular response as the contrast gain control equation

$$R_B = \frac{(c_L + c_R)^p}{Z + (c_L + c_R)^q}, \quad (9)$$

where the binocular response of the model (R_B) is defined as the sum of monocular inputs (c_L and c_R) raised to the power p normalized by the sum of monocular inputs raised to the power q and where ($p > q$). The parameter Z prevents division by zero. The model can now generate responses at the harmonic frequencies for stimuli presented in temporal phase under On/Off flicker (see Figure 5 and Table 1). While this model iteration improves on the fits, it nevertheless struggles to fit SNR values at the fundamental frequency (3Hz) and is, as with the linear summation model, incapable of generating responses to stimuli presented with On/Off flicker in temporal anti-phase; the linear sum of stimuli presented in temporal anti-phase will always return zero. The model, therefore, still lacks the necessary architecture to adequately define neural responses to our stimuli.

The Two-Stage Contrast Gain Control Model

The simple models described above could not accurately represent the observer SSVEPs we recorded. They overestimated SNRs at the fundamental frequency and failed to generate responses for stimuli presented in temporal anti-phase with On/Off flicker. A potential refinement to the model is add a monocular transducer prior to binocular combination Baker

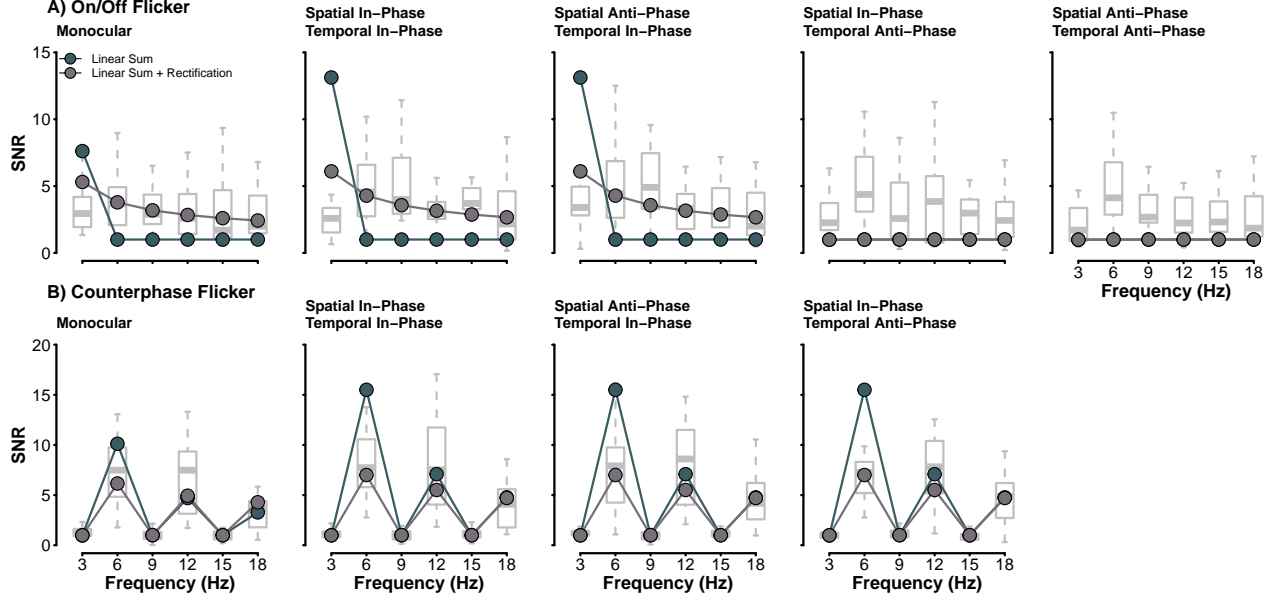


Figure 5: Fits of the linear sum (green) and the rectified linear sum (brown) models. Boxplots behind model responses show the distribution of observer SNRs. Model SNRs were fit to the median SNR of observers, which is represented by the thicker line within the box.

et al. (2018). The architecture of this model now begins with a monocular stage

$$r_L = \frac{c_L^m}{S + c_L}, \quad r_R = \frac{c_R^m}{S + c_R} \quad (10)$$

where a non-linearity (m) is applied to the monocular inputs (c_L and c_R) in addition to self-suppression. The outputs of the monocular stage are then fed into a binocular stage that undergoes a second contrast gain control,

$$R_B = \frac{(r_L + r_R)^p}{Z + (r_L + r_R)^q}. \quad (11)$$

In this model variant, m is the monocular excitatory component and determines the extent of summation at detection threshold, moderated by the suppressive term. In the second stage, $p > q$ as with Equation 9, which is necessary to capture the facilitative effects of dichoptic masking (Meese et al., 2006). We can strengthen the normalization of the monocular input by adding interocular suppression and replacing Equation 10 (the first stage) with

$$r_L = \frac{c_L^m}{S + c_L + c_R}, \quad r_R = \frac{c_R^m}{S + c_R + c_L}. \quad (12)$$

This model iteration is identical to the two-stage contrast gain control model defined by Meese et al. (2006).

The fits of both model variants, with and without interocular suppression, are shown in Figure 6. The difference in their quality is negligible (see Table 1) as both describe most experimental conditions well. The addition of the monocular transducer enables the model to

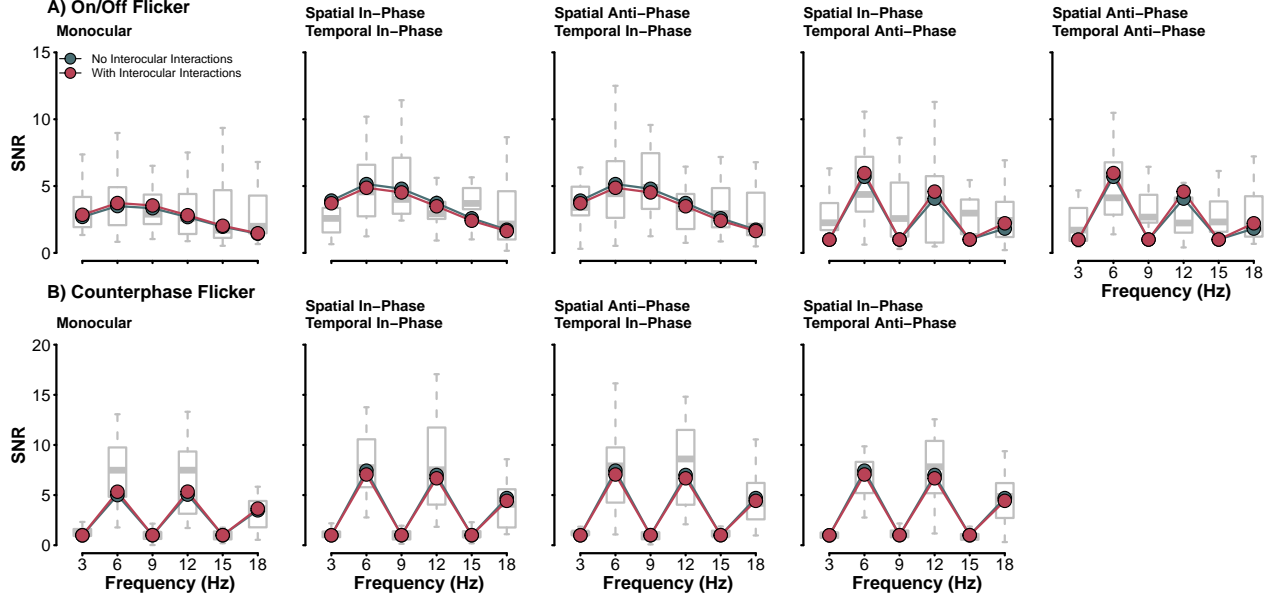


Figure 6: Fits of the two-stage contrast gain control model without (green) and with (red) interocular suppression. Boxplots behind model responses show the distribution of observer SNRs. Model SNRs were fit to the median SNR of observers, which is represented by the thicker line within the box.

fit observer SNRs at the fundamental frequency for stimuli presented in temporal phase under On/Off flicker and importantly, it now generates responses for stimuli presented in temporal anti-phase. The transduced monocular inputs no longer cancel each other at the binocular stage. While the model can generate responses to temporal anti-phase stimuli, it only does so at the even-harmonics (2F-6Hz, 4F-12Hz, and 6F-18Hz) of the SSVEP spectrum. This is to be expected as the model can only generate binocular responses; it does not preserve monocular signals beyond the first stage. As the two rectified sine waves are in anti-phase, their sum will generate a new waveform with frequencies at twice the frequency of the original (6Hz) and its integer harmonics (2F-12Hz and 3F-18Hz). The responses we recorded at the fundamental frequency (3Hz) and its odd integer harmonics (3F - 9Hz, 5F - 15Hz) cannot be explained by ab architecture with a purely binocular output. Next, we explore methods of preserving the monocular signal in an effort to explain observer responses to stimuli presented in temporal anti-phase.

Parallel Monocular and Phase-Selective Channels

Observer SNRs for stimuli presented in temporal anti-phase contain a binocular and monocular response to stimuli. To preserve the monocular response in the modelling, we add parallel monocular channels to the two-stage contrast gain control model, similar to Georgeson et al. (2016). These channels are fully monocular and do not include interocular suppression,

$$\mu_L = \frac{C_L^m}{S + C_L}, \quad \mu_R = \frac{C_R^m}{S + C_R}. \quad (13)$$

In this equation, μ_L is the output of the first stage of the monocular channel for the left eye, and μ_R is that of the right eye. The excitatory exponent m is identical to that in the

channels that include binocular interaction (see Equation 12). The output of the monocular channels undergoes a second contrast gain control stage identical to that of the binocular channel,

$$R_{\mu_L} = \frac{\mu_L^p}{Z + \mu_L^q}, \quad R_{\mu_R} = \frac{\mu_R^p}{Z + \mu_R^q}. \quad (14)$$

R_{μ_L} and R_{μ_R} represent the final responses of the left and right monocular channels. No additional free parameters are included in the model with parallel monocular channels; the parameters m , p , q , S and Z used to define the monocular channel responses are identical to those of the binocular channels.

The inclusion of parallel monocular channels poses an interesting problem in our modelling as we now contend with three visual cues from which to generate model SSVEPs: monocular left (R_L), monocular right (R_R), and binocular (R_B). Psychophysically, cue selection has been implemented as a Minkowski sum with a very large (≈ 30) exponent (Georgeson et al., 2016), approximating a MAX rule. This method is inappropriate when modelling neural data as the recordings from the scalp represent an amalgamation of all channel cues generated by the stimuli (Wade and Baker, 2025). Our model output must therefore represent the combination of signals instead of the selection of the strongest signal. Here, it is implemented as the sum of the Fourier amplitude spectra of all three channel outputs. This sum preserves the amplitude responses required to generate SSVEPs and prevents the nullifying of responses from summing signals in anti-phase.

Preserving monocular responses until the output stage with parallel monocular channels improved the fits to our data (see Table 1 and Figure 7). The model now captures responses at the fundamental (3Hz) and odd-integer harmonics (9Hz and 15Hz) of the temporal anti-phase conditions under On/Off flicker. Monocular signals, while weaker than binocular signals, are preserved in the neural responses of observers and thus must be accounted for in their computational description. Parallel monocular channels, as defined by Georgeson et al. (2016) appear to be an adequate descriptor of monocular signals.

Psychophysically, spatial phase has a meaningful impact on binocular combination (Bacon, 1976; Baker and Meese, 2007; Simmons, 2005) and the two-stage contrast gain control often includes phase-selective channels to account for these effects. In our study, we find little evidence of any influence of spatial phase on observer SSVEPs as no statistically significant difference in signal-to-noise ratios across spatial phase were found. Still, we opt it prudent to verify if the addition of phase-selective channels improves the fits of the model to our data. Phase-selectivity was added to the binocular and monocular channels by replicated the equations of the first and second stage, for a total of six channels (see Figure 4). As with the previous model, no additional model parameters were required to include phase-selectivity; the parameters m , p , q , S and Z used to define the responses of all six channels in this model.

Model responses were generated from sine waves (in temporal phase or anti-phase) fed into their respective positive or negative phase channels. This simulated the spatial phase of stimuli presented to observers. We refer to this model iteration as the full model as it includes a binocular channel with a monocular stage (with interocular interactions), a binocular stage, parallel monocular channels (with their respective stages), and phase-selectivity. This is, in

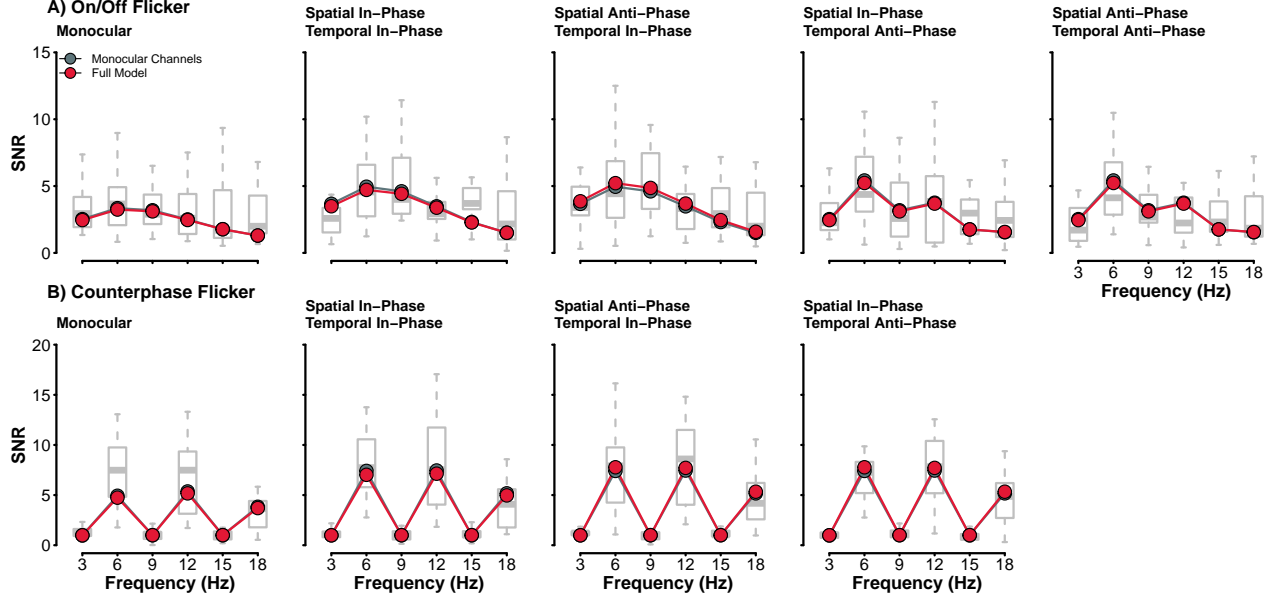


Figure 7: Fits of the two best performing models to our observer data. Both models, that including parallel monocular channels and the full model with the added phase-selective channels perform quite similarly.

essence, the 6-channel 2-cue model proposed by Georgeson et al. (2016) to explain binocular combination under multiple experimental conditions. As with the addition of monocular channels, including phase-selectivity to the model means that we now have six final signals to contend with: a binocular and two monocular channels selective for positive spatial phase and a binocular and two monocular channels selective for negative spatial phase. We utilized the same method of combining signal as above: we first sum the Fourier amplitude spectra of observers across the positive and negative phase-selective channels and then combine the binocular and monocular channels. The inclusion of phase-selectivity did not improve model fits. The R^2 value calculated across the 6 frequencies and 9 experimental conditions was no different than that of the previous model (see Table 1) which indicates that the spatial phase of stimuli does not have a meaningful impact on the SSVEP amplitudes of observers.

Discussion

The computational architecture of binocular combination, under the two-stage contrast gain control model framework, has been carefully evaluated on psychophysical data (Baker and Meese, 2007; Georgeson et al., 2016; Meese et al., 2006), yet its ability to explain neural data has only been explored on a limited set of stimulus conditions (Lygo et al., 2021; Richard et al., 2018). In this study, we investigated the effects of stimulus spatial and temporal phase on observer SSVEPs and explored the ability of the two-stage contrast gain control model - and its variants - to capture our neural data. On/Off flicker generated responses at the fundamental frequency (3Hz) and its harmonics (6Hz, 9Hz, 12Hz, and 15Hz) while counterphase flicker generated responses at twice the fundamental frequency (6Hz) and its even integer harmonics (12Hz and 18Hz). No statistically significant difference was found be-

tween the monocular and binocular conditions presented either with On/Off or counterphase flicker. This is consistent with ocularity invariance; binocular and monocular stimuli are judged equal in magnitude at high contrast (Baker et al., 2018; Legge, 1984; Maehara and Goryo, 2005; Meese et al., 2006). We additionally found no statistically significant differences in SSVEPs for all stimulus conditions under counterphase flicker.

Presenting stimuli in temporal anti-phase reduced the magnitude of responses at the fundamental frequency (3Hz) in comparison to its temporal phase counterpart, but was not abolished. This finding indicates that, even under binocular viewing, monocular signals can be measured at the scalp with SSVEPs. This was confirmed in our modelling as only the two-stage contrast gain control model with parallel monocular channels, which preserve monocular signals throughout the model architecture, was able to accurately capture the data in all experimental conditions. Simpler models failed to generate the necessary responses at the fundamental and odd-integer harmonics for stimuli presented in temporal anti-phase while a more complex model that included phase-selectivity did not improve the quality of fits. Overall, we find that the same general framework that has been used to explain psychophysical stimulus combination can be successfully applied to neural data collected under a variety of experimental conditions.

Monocular signals

It has long been assumed by most computational descriptions of binocular combination that only the binocular response was available to later stages of perception and decision (Baker and Meese, 2007; Ding et al., 2013; Ding and Sperling, 2006; Legge, 1984; Meese et al., 2006). The monocular pathways, which represent the early stages of the visual processing stream, only serve as the input to combine. However, psychophysical evidence from adaptation and discrimination experiments have demonstrated that monocular signals do contribute to perception (Blake et al., 1981; Georgeson et al., 2016; Moulden, 1980) and that monocular channels parallel to the binocular channel should be included in models of binocular combination. In this study, we found monocular responses to stimuli can be recorded with SSVEPs under binocular stimulation. Presenting stimuli in temporal anti-phase under On/Off flicker generates two transients per cycle and a binocular system, which combines the monocular inputs of each eye, would only generate responses at 6Hz. While the 6Hz component was large, we still found SSVEPs at 3Hz that exceeded the noise level in our data. These 3Hz components represent the individual oscillations for each eye and are therefore likely representative of a monocular response. The reduction in response magnitude of the 3Hz component we observed from the temporal in-phase conditions to the temporal anti-phase can thus be explained as the transition from a binocular to a, inadvertently weaker, monocular response.

Computationally, we demonstrated that many mechanisms of binocular combination, including monocular non-linearities, interocular interactions, and parallel monocular channels were required to explain the SNR spectra of our observers. Parallel monocular channels were particularly important in capturing observer data in the two temporal anti-phase conditions presented with On/Off flicker. Without the addition of these channels, the models could not generate a response at the fundamental (3Hz) or its odd integer harmonics. While an important inclusion to our study, the addition of monocular channels did not meaningfully

alter the ability of the two-stage contrast gain control model to capture observer SNRs in the other experimental conditions. Monocular contributions to the model output are largest when the stimulus contrast between the two eyes differ (Georgeson et al., 2016), experimental scenarios that we did not explore here.

Spatial Phase

Our results did not suggest a impact of stimulus spatial phase on observer SSVEPs. It is well-known that spatial phase affects binocular combination when measured psychophysically (Bacon, 1976; Baker and Meese, 2007; Simmons, 2005). The binocular combination of two opposite polarity stimuli does not cancel; it sums, and thus influences sensitivity to the stimuli. It is therefore odd to find little to no influence of spatial phase on the SSVEPs of observers, particularly as SSVEP amplitude is associated with perceptual sensitivity (Bosse et al., 2018; Campbell and Kulikowski, 1972; Campbell and Maffei, 1970; Norcia et al., 2015). The absence of a clear spatial phase effect also complicates our ability to describe the contributions of a differencing channel in our study (Chen and Li, 1998; May et al., 2012; May and Zhaoping, 2016).

Spatial phase-dependent effects in SSVEPs have been recorded with motion stimuli (Cottetereau et al., 2014; Kohler et al., 2018). The dichoptic presentation of moving bars, whereby they either move in-phase (lateral motion) or in anti-phase (motion-in-depth), impacts the amplitude of SSVEPs. In-phase motion generates SSVEP amplitudes that are twice those of motion in anti-phase (Cottetereau et al., 2014). A difference response can also be recorded for dichoptic stimuli when they are frequency tagged (Katyal et al., 2018; Sutoyo and Srinivasan, 2009) where the “conflict” response is represented at the intermodulation frequencies. All stimuli in this study were presented at 3Hz, we did not frequency tag stimuli presented to the left and right eye. Thus, the responses we recorded at the scalp are a spatial aggregation of the stimuli presented to observers (Wade and Baker, 2025). Spatially aggregated responses will be identical regardless of stimulus phase and thus generate phase-insensitive responses.

Conclusion

We investigated the effects of stimulus spatial and temporal phase on observer SSVEPs and explored the necessary computational components to explain our data. We worked under the framework of the two-stage contrast gain control model of binocular vision (Meese et al., 2006) and explored the impact of interocular interactions, parallel monocular channels, and phase-selective channels on the fits of the model to our data. The largest effect to capture was the presence of odd-integer harmonics in the temporal anti-phase conditions, which represents the monocular response to stimuli and was well-explained by the addition of parallel monocular channels to the model. The two-stage contrast gain control model of binocular combination remains a powerful descriptor of binocular vision as it can explain a large variety experimental conditions and modalities (psychophysics and neuroimaging).

Data and Code Availability

We provide the raw (.cnt) and processed (.RData) observer SSVEPs and all code used in this study have been made available on the Open Science Framework and can be accessed using the following project link: <https://osf.io/cn894/>.

References

- Bacon, J.H., 1976. The interaction of dichoptically presented spatial gratings. *Vision Res* 16, 337–44. [https://doi.org/10.1016/0042-6989\(76\)90193-0](https://doi.org/10.1016/0042-6989(76)90193-0)
- Baker, D.H., Lygo, F.A., Meese, T.S., Georgeson, M.A., 2018. Binocular summation revisited: Beyond $\sqrt{2}$. *Psychol Bull* 144, 1186–1199. <https://doi.org/10.1037/bul0000163>
- Baker, D.H., Meese, T.S., 2007. Binocular contrast interactions: Dichoptic masking is not a single process. *Vision Res* 47, 3096–107. <https://doi.org/10.1016/j.visres.2007.08.013>
- Baker, D.H., Meese, T.S., Georgeson, M.A., 2007a. Binocular interaction: Contrast matching and contrast discrimination are predicted by the same model. *Spat Vis* 20, 397–413. <https://doi.org/10.1163/156856807781503622>
- Baker, D.H., Meese, T.S., Hess, R.F., 2008. Contrast masking in strabismic amblyopia: Attenuation, noise, interocular suppression and binocular summation. *Vision Res* 48, 1625–40. <https://doi.org/10.1016/j.visres.2008.04.017>
- Baker, D.H., Meese, T.S., Summers, R.J., 2007b. Psychophysical evidence for two routes to suppression before binocular summation of signals in human vision. *Neuroscience* 146, 435–448. <https://doi.org/10.1016/j.neuroscience.2007.01.030>
- Baker, D.H., Wade, A.R., 2017. Evidence for an optimal algorithm underlying signal combination in human visual cortex. *Cereb Cortex* 27, 254–264. <https://doi.org/10.1093/cercor/bhw395>
- Blake, R., 1989. A neural theory of binocular rivalry. *Psychol Rev* 96, 145–67. <https://doi.org/10.1037/0033-295x.96.1.145>
- Blake, R., Overton, R., Lema-Stern, S., 1981. Interocular transfer of visual aftereffects. *J Exp Psychol Hum Percept Perform* 7, 367–81. <https://doi.org/10.1037/0096-1523.7.2.367>
- Blake, R., Wilson, H., 2011. Binocular vision. *Vision Research* 51, 754–770. <https://doi.org/10.1016/j.visres.2010.10.009>
- Bosse, S., Acqualagna, L., Samek, W., Porbadnigk, A.K., Curio, G., Blankertz, B., Müller, K.-R., Wiegand, T., 2018. Assessing perceived image quality using steady-state visual evoked potentials and spatio-spectral decomposition. *IEEE Transactions on Circuits and Systems for Video Technology* 28, 1694–1706. <https://doi.org/10.1109/TCSVT.2017.2694807>
- Campbell, F.W., Green, D.G., 1965. Monocular versus binocular visual acuity. *Nature* 208, 191–2. <https://doi.org/10.1038/208191a0>
- Campbell, F.W., Kulikowski, J.J., 1972. The visual evoked potential as a function of contrast of a grating pattern. *J Physiol* 222, 345–56. <https://doi.org/10.1113/jphysiol.1972.sp009801>
- Campbell, F.W., Maffei, L., 1970. Electrophysiological evidence for the existence of orientation and size detectors in the human visual system. *J Physiol* 207, 635–52. <https://doi.org/10.1113/jphysiol.1970.sp009085>

- Chatrian, G.E., Lettich, E., Nelson, P.L., 1985. Ten percent electrode system for topographic studies of spontaneous and evoked EEG activities. *American Journal of EEG Technology* 25, 83–92. <https://doi.org/10.1080/00029238.1985.11080163>
- Chen, D., Li, Z., 1998. A psychophysical experiment to test the efficient stereo coding theory, in: Wong, K.-Y.M., King, I., Yeung, D.Y. (Eds.), *Theoretical Aspects of Neural Computation: A Multidisciplinary Perspective*. Springer Verlag, New York, pp. 225–235.
- Cottareau, B.R., McKee, S.P., Norcia, A.M., 2014. Dynamics and cortical distribution of neural responses to 2D and 3D motion in human. *Journal of Neurophysiology* 111, 533–543. <https://doi.org/10.1152/jn.00549.2013>
- Delorme, A., Makeig, S., 2004. EEGLAB: An open source toolbox for analysis of single-trial EEG dynamics including independent component analysis. *Journal of Neuroscience Methods* 134, 9–21. <https://doi.org/10.1016/J.JNEUMETH.2003.10.009>
- Ding, J., Klein, S.A., Levi, D.M., 2013. Binocular combination of phase and contrast explained by a gain-control and gain-enhancement model. *J Vis* 13, 13. <https://doi.org/10.1167/13.2.13>
- Ding, J., Sperling, G., 2006. A gain-control theory of binocular combination. *Proc Natl Acad Sci U S A* 103, 1141–6. <https://doi.org/10.1073/pnas.0509629103>
- Georgeson, M.A., Wallis, S.A., Meese, T.S., Baker, D.H., 2016. Contrast and lustre: A model that accounts for eleven different forms of contrast discrimination in binocular vision. *Vision Research* 129, 98–118. <https://doi.org/10.1016/j.visres.2016.08.001>
- Hansen, B.C., Hess, R.F., 2006. Discrimination of amplitude spectrum slope in the fovea and parafovea and the local amplitude distributions of natural scene imagery. *J Vis* 6, 696–711. <https://doi.org/10.1167/6.7.3>
- Heeger, D.J., 1992. Normalization of cell responses in cat striate cortex. *Vis Neurosci* 9, 181–97. <https://doi.org/10.1017/s0952523800009640>
- Katyal, S., Vergeer, M., He, S., He, B., Engel, S.A., 2018. Conflict-sensitive neurons gate interocular suppression in human visual cortex. *Scientific Reports* 8, 1239. <https://doi.org/10.1038/s41598-018-19809-w>
- Kohler, P.J., Meredith, W.J., Norcia, A.M., 2018. Revisiting the functional significance of binocular cues for perceiving motion-in-depth. *Nature Communications* 9, 3511. <https://doi.org/10.1038/s41467-018-05918-7>
- Legge, G.E., 1984. Binocular contrast summation–i. Detection and discrimination. *Vision Res* 24, 373–83. [https://doi.org/10.1016/0042-6989\(84\)90063-4](https://doi.org/10.1016/0042-6989(84)90063-4)
- Lygo, F.A., Richard, B., Wade, A.R., Morland, A.B., Baker, D.H., 2021. Neural markers of suppression in impaired binocular vision. *Neuroimage* 230, 117780. <https://doi.org/10.1016/j.neuroimage.2021.117780>
- Maehara, G., Goryo, K., 2005. Binocular, monocular and dichoptic pattern masking. *Optical Review* 12, 76–82. [https://doi.org/DOI 10.1007/s10043-004-0076-5](https://doi.org/DOI%2010.1007/s10043-004-0076-5)
- May, K.A., Zhaoping, L., 2016. Efficient coding theory predicts a tilt aftereffect from viewing untilted patterns. *Curr Biol* 26, 1571–1576. <https://doi.org/10.1016/j.cub.2016.04.037>
- May, K.A., Zhaoping, L., Hibbard, P.B., 2012. Perceived direction of motion determined by adaptation to static binocular images. *Curr Biol* 22, 28–32. <https://doi.org/10.1016/j.cub.2011.11.025>
- Meese, T.S., Baker, D.H., 2011. Contrast summation across eyes and space is revealed along the entire dipper function by a “swiss cheese” stimulus. *J Vis* 11, 1–23. <https://doi.org/10.1167/11.1.1>

- [//doi.org/10.1167/11.1.23](https://doi.org/10.1167/11.1.23)
- Meese, T.S., Georgeson, M.A., Baker, D.H., 2006. Binocular contrast vision at and above threshold. *Journal of vision* 6, 1224–1243. <https://doi.org/10.1167/6.11.7>
- Moradi, F., Heeger, D.J., 2009. Inter-ocular contrast normalization in human visual cortex. *J Vis* 9, 13 1–22. <https://doi.org/10.1167/9.3.13>
- Moulden, B., 1980. After-effects and the integration of patterns of neural activity within a channel. *Philos Trans R Soc Lond B Biol Sci* 290, 39–55. <https://doi.org/10.1098/rstb.1980.0081>
- Norcia, A.M., Appelbaum, L.G., Ales, J.M., Cottareau, B.R., Rossion, B., 2015. The steady-state visual evoked potential in vision research: A review. *Journal of Vision* 15, 4. <https://doi.org/10.1167/15.6.4>
- Regan, M., Regan, D., 1988. A frequency domain technique for characterizing nonlinearities in biological systems. *Journal of theoretical biology* 133, 293–317.
- Richard, B., Chadnova, E., Baker, D.H., 2018. Binocular vision adaptively suppresses delayed monocular signals. *Neuroimage* 172, 753–765. <https://doi.org/10.1016/j.neuroimage.2018.02.021>
- Simmons, D.R., 2005. The binocular combination of chromatic contrast. *Perception* 34, 1035–1042. <https://doi.org/10.1068/p5279>
- Simmons, D.R., Kingdom, F.A.A., 1998. On the binocular summation of chromatic contrast. *Vision Research* 38, 1063–1071. [https://doi.org/10.1016/S0042-6989\(97\)00272-1](https://doi.org/10.1016/S0042-6989(97)00272-1)
- Sutoyo, D., Srinivasan, R., 2009. Nonlinear SSVEP responses are sensitive to the perceptual binding of visual hemifields during conventional “eye” rivalry and interocular “percept” rivalry. *Brain Research* 1251, 245–255. <https://doi.org/https://doi.org/10.1016/j.brainres.2008.09.086>
- Tadmor, Y., Tolhurst, D.J., 1994. Discrimination of changes in the second-order statistics of natural and synthetic images. *Vision Research* 34, 541–554. [https://doi.org/10.1016/0042-6989\(94\)90167-8](https://doi.org/10.1016/0042-6989(94)90167-8)
- Wade, A.R., Baker, D.H., 2025. Measuring contrast processing in the visual system using the steady state visually evoked potential (SSVEP). *Vision Research* 231, 108614. <https://doi.org/10.1016/j.visres.2025.108614>
- Wilson, H.R., 2003. Computational evidence for a rivalry hierarchy in vision. *Proceedings of the National Academy of Sciences of the United States of America* 100, 14499–14503. <https://doi.org/10.1073/pnas.2333622100>